

Properties of polyacetylene doped with I, Br, IrCl₆, and FeCl₃

E. K. Sichel, M. F. Rubner, and S. K. Tripathy

GTE Laboratories, Inc., 40 Sylvan Road, Waltham, Massachusetts 02254

(Received 11 June 1982)

We have studied the temperature dependence of the resistivity of polyacetylene doped with I, Br, IrCl₆, and FeCl₃. The roles of dopant molecule size, doping technique, doping speed, and isomerization state in determining the mechanism of electrical conduction are discussed. Evidence for dopant-induced disorder is presented from x-ray and high-resolution transmission electron microscopy studies. We suggest that the dopant molecule size determines whether the dopant is dispersed molecularly or whether the dopant molecules aggregate. In addition, we find significant differences in the activation energy, $k_B T_0$, between CH(Br)_y and CH(I)_y, although the characteristic temperature dependence of the resistivity is the same.

I. INTRODUCTION

One of the outstanding controversies about polyacetylene concerns dopant homogeneity. There are at least three types of inhomogeneities which have been discussed: a dopant concentration gradient from the surface to the center of a sample,¹ a radial concentration gradient of dopant from the surface to the center of the nominally 200-Å-diameter polyacetylene fibrils,² and an aggregation of dopant molecules on a scale ≤ 200 Å so that the dopant is not dispersed throughout the sample as uniformly separated individual molecules.³ In this paper, we discuss the third type of dopant distribution and how it is influenced by method of sample preparation, dopant molecule species, dopant molecule size, and dopant uptake.

In Sec. II, we discuss sample preparation; Sec. III concerns the mechanism of electrical transport. Section IV concerns materials characterization by transmission electron microscopy (TEM), x-ray diffraction, and optical absorption. Our thesis is that the dopant molecule size determines whether the dopant is dispersed molecularly or not. Evidence is drawn from $\rho(T)$ studies and electron micrographs on our prototype small molecule I and large molecule IrCl₆. In addition, we show that two similar dopants, iodine and bromine, give vastly different carrier activation energies. All dopants treated here are electron acceptors.

II. SAMPLE PREPARATION

Polyacetylene was prepared according to the method of Wnek *et al.*⁴ The resultant gel was pressed into free standing films of ca. 0.04 cm

thickness. Polymerizations were carried out at -78°C which results in the predominantly *cis*-isomer (80–95%) of polyacetylene. *Trans*-polyacetylene was prepared by thermal isomerization (for 20 min at 160°C) of *cis*-polyacetylene in a vacuum-sealed tube. Elemental analysis of the polyacetylene gel indicates analytical purity (typical analysis: 90.2 wt. % C, 8.21 wt. % H). Details of the morphology, microstructure, and materials characterization of polyacetylene gels have been published in our earlier work.⁵ Micrographs of our gel polyacetylene are discussed in Sec. IV. The structure closely resembles that of the Shirakawa preparation of films of polyacetylene. We have not noted any difference in electrical properties of our gel material compared to film material reported by other workers. The density of the gel polyacetylene is lower and may lower the absolute value of the bulk electrical conductivity of the gel for a given weight percent dopant.

In order to obtain optical measurements, it was necessary to polymerize thin films of polyacetylene on quartz substrates. This was accomplished using techniques similar to those described by Shirakawa and Ikeda.⁶ Absorption measurements utilizing these thin films were made on a Cary 17 spectrophotometer.

Dihydrogenhexachloroiridate ($\text{H}_2\text{IrCl}_6 \cdot 6\text{H}_2\text{O}$), iodine, bromine, and ferric chloride (FeCl_3) were used as received. All manipulations of dopants were carried out using vacuum line techniques or in an inert atmosphere. The various procedures used to dope polyacetylene (slow doping, solution doping, etc.) have been described in previous publications.⁵ In this work, we added the additional refinement of solution doping with dihydrogenhexachloroiridate

in a 90/10 vol % solution of nitromethane—acetic acid. The acetic acid was added to prevent impurities from precipitating out of the doping solution and onto the polyacetylene film.

Attempts were made to dope with chlorine, a small molecule of the halogen series; however, even under dilute doping conditions it was not possible to prevent chlorine addition across the double bonds of polyacetylene.

III. MECHANISM OF ELECTRICAL TRANSPORT

The mechanism of electrical conduction in doped polyacetylene is controversial. There are at least three dopant regimes: (1) at dopant levels below 0.003 mole fraction, phonon-assisted hopping between soliton bound states in *trans*-polyacetylene has been proposed⁷; (2) above a critical dopant concentration, metallic conductivity has been proposed⁸; (3) two conduction models have been proposed for polyacetylene in the semiconducting regime for dopant mole fraction $y > 0.003$. This is the regime considered in this work. The first is a variable range hopping of the type described by Mott⁹ in which

$$\rho = \rho_0 \exp(T_0/T)^{1/4}. \quad (1)$$

We have reported¹⁰ that the resistivity of both *cis*-CH(I)_y and *cis*-CH(Br)_y fits an expression of that kind over a wide temperature range. Other workers have reported the same temperature dependence of ρ in films of CH(I)_y and CH(Br)_y.^{11,12} The model of Mott requires that carriers hop between molecularly dispersed dopant sites in such a way as to minimize the energy required for the hop. T_0 depends on the extent of the localized wave function, $1/\alpha$, and the density of states at the Fermi level, N , and may be written

$$T_0 \propto \alpha^3/N. \quad (2)$$

The second model of conduction assumes that the dopant molecules cluster together forming conducting islands $< 200 \text{ \AA}$ in diameter.³ In such a case, the addition of a carrier to a conducting island changes the energy of the system because of the capacitive charging energy. There are two theoretical formulations of the problem, both of which were developed to describe conduction in granular metals. Sheng's¹³ analysis assumes a distribution of island sizes and includes a detailed calculation of the temperature, electric field, and composition dependence of the conductivity. Simanek's¹⁴

analysis put fewer constraints on the island size distribution but calculates only the temperature dependence of the conductivity. For both models, the resistivity is a function of the form

$$\rho = \rho_0 \exp(T_0/T)^{1/2}. \quad (3)$$

We have previously reported¹⁰ that the resistivity of CH(IrCl₆)_y follows Eq. (3). Others³ have found the same behavior in films of CH(AsF₅)_y. Our work is an effort to understand why the resistivity of CH(I)_y and CH(Br)_y follows Eq. (1), whereas the resistivity of CH(AsF₅)_y and CH(IrCl₆)_y follows Eq. (3). Among the variables we considered are doping speed and technique.

We examined $\rho(T)$ of I- and Br-doped samples of *cis*-polyacetylene for both vapor and solution doping and found the results to be identical. In spite of rapid doping there was no evidence for dopant aggregation into islands as seen in the $\rho(T)$ data. There is, however, a significant difference between iodine- and bromine-doped *cis*-polyacetylene in the activation energy $k_B T_0$ from Eq. (2). For the same value of y , the values of T_0 are about 2 orders of magnitude higher for CH(I)_y than for CH(Br)_y, as shown in Figs. 1 and 2. The break in each curve represents the metal-to-semiconducting transition at the critical concentration of dopant y . Note that the resistivity in the metallic regime is not truly metallic and temperature independent but remains (weakly) thermally activated. Figure 3 is an example of the $\rho(T)$ data from which T_0 was calculated. The difference in slope of $\log_{10} \rho$ vs $T^{-1/4}$ for iodine and bromine can be seen in the raw data. All starting materials were *cis*-polyacetylene.

Chiang *et al.*¹¹ have reported $\rho(T)$ data from $T = 110 - 300 \text{ K}$ for films of CH(I)_y and CH(Br)_y. They found good agreement in the slope of the $\log_{10} \rho$ -vs- $T^{-1/4}$ curves for the two dopants for the same values of y in contrast to our results. They

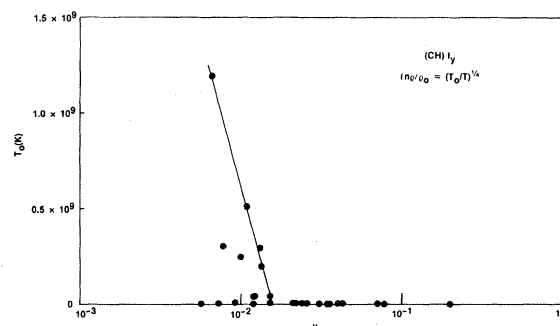


FIG. 1. Activation energy of iodine-doped polyacetylene as a function of dopant concentration.

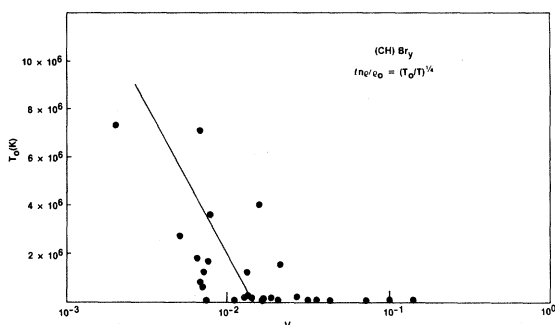


FIG. 2. Activation energy of bromine-doped polyacetylene as a function of dopant concentration.

also noted that Br adds across the polyacetylene double bond and causes the resistivity of $\text{CH}(\text{Br})_y$ to be higher than $\text{CH}(\text{I})_y$ for the same y , in contrast to our results. We believe the two effects are related, and it suggests that differing dopant-polyacetylene reactions account for the disagreement between their data and ours. Epstein *et al.*¹² have reported $T_0 = 3 \times 10^6$ K for film $\text{CH}(\text{I})_{0.01}$, which is comparable to our $\text{CH}(\text{Br})_{0.01}$ samples but in disagreement with our value of T_0 for $\text{CH}(\text{I})_{0.01}$, again suggesting that T_0 is sensitive to dopant-polymer interaction.

The value of T_0 depends, as shown in Eq. (2), on the extent of the localized wave function as well as on the density of states at the Fermi level N . We expect N to be controlled by y , so for the same value

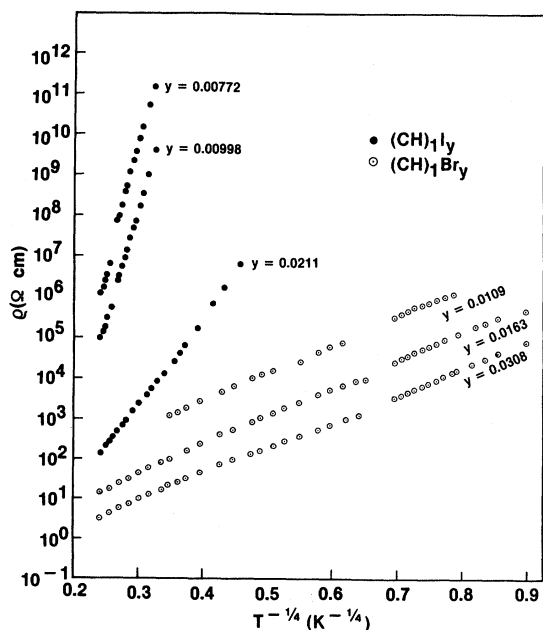


FIG. 3. Resistivity of $(\text{CH})\text{I}_y$ and $(\text{CH})\text{Br}_y$ as a function of $T^{-1/4}$ for several values of dopant concentration y .

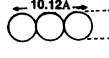

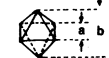
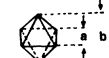

of y , both $\text{CH}(\text{I})_y$ and $\text{CH}(\text{Br})_y$ should have the same N . It has been pointed out by several authors¹⁵ that the dopant includes both I_3^- and I_5^- . It is possible that the $\text{I}_5^-:\text{I}_3^-$ ratio is different from the $\text{Br}_5^-:\text{Br}_3^-$ ratio. In the most extreme case, however, the effective N for I could be smaller by no more than a factor of $\frac{3}{5}$ than the effective N for Br. Therefore, the large difference in T_0 cannot be accounted for by N .

If we attribute the difference in T_0 to the extent of the localized wave function $1/\alpha$, then we must assume a large difference in the environment in which the electron acceptor sits. The I (or I_3^- or I_5^-) atom is larger than the Br (or Br_3^- or Br_5^-) and might cause more disorder in the polymer. A comparison of dopant molecule sizes is shown in Table I.

Figure 4 shows an electron micrograph, at high magnification, of iodine-doped polyacetylene. The dopant level is estimated to be above the metal-to-semiconductor transition. Note that the nominally 200-Å fibrils are well defined in the image, but there is no evidence of structure due to dopant molecules clustering together.

The case of IrCl_6 dopant, on the other hand, shows evidence of dopant inhomogeneity, as shown in Fig. 5. There are two scales of dopant inhomogeneity revealed in the figure. The first type of inhomogeneity is a collection of 15-Å-diameter closely-spaced black dots indicated by arrow B. The second is the collection of ≈ 300 -Å-diameter black islands dispersed throughout the fibrils indicated by two arrow A's. Discussed in Sec. IV, these represent regions of crystallinity different from the

TABLE I. Dopant molecule sizes and shapes. For further details, see Ref. 10.

DOPANT	STRUCTURE	DIMENSIONS
I I_3^-	LINEAR CHAIN 	$a = 3.37\text{Å}$
Br Br_3^-	LINEAR CHAIN 	$a = 3.00\text{Å}$
IrCl_6^{-2}	OCTAHEDRON 	$a = 6.08\text{Å}$ $b = 8.6\text{Å}$
AsF_6^{-1}	OCTAHEDRON 	$a = 4.41\text{Å}$ $b = 6.24\text{Å}$
FeCl_4^{-2}	TETRAHEDRON 	$a = 7.05\text{Å}$

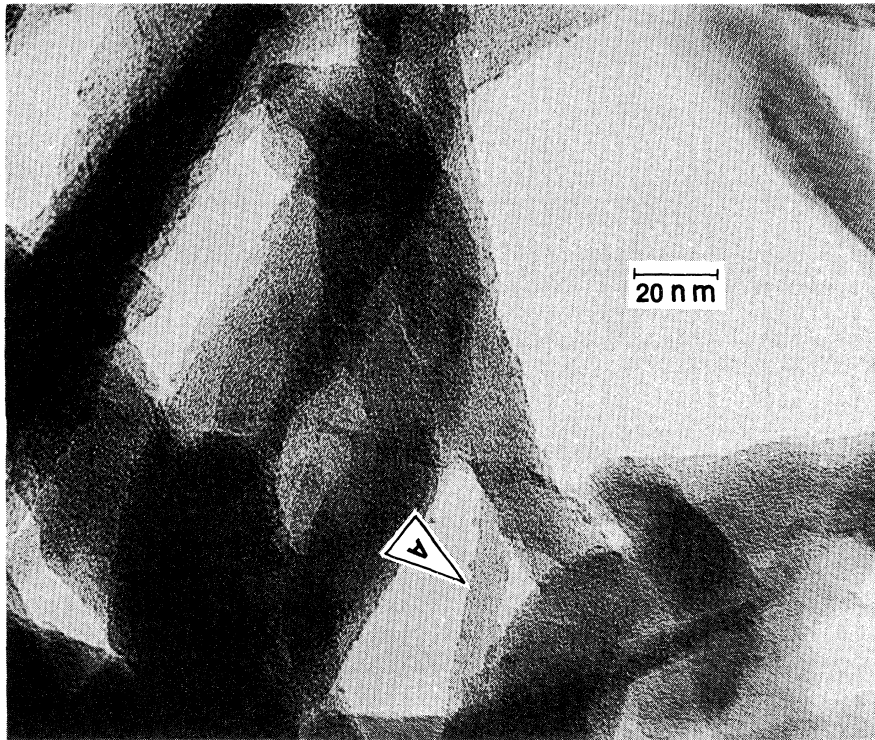


FIG. 4. High-resolution and -magnification electron micrograph of heavily doped CH(I) , showing no evidence of dopant aggregation. Arrow indicates single fibril.

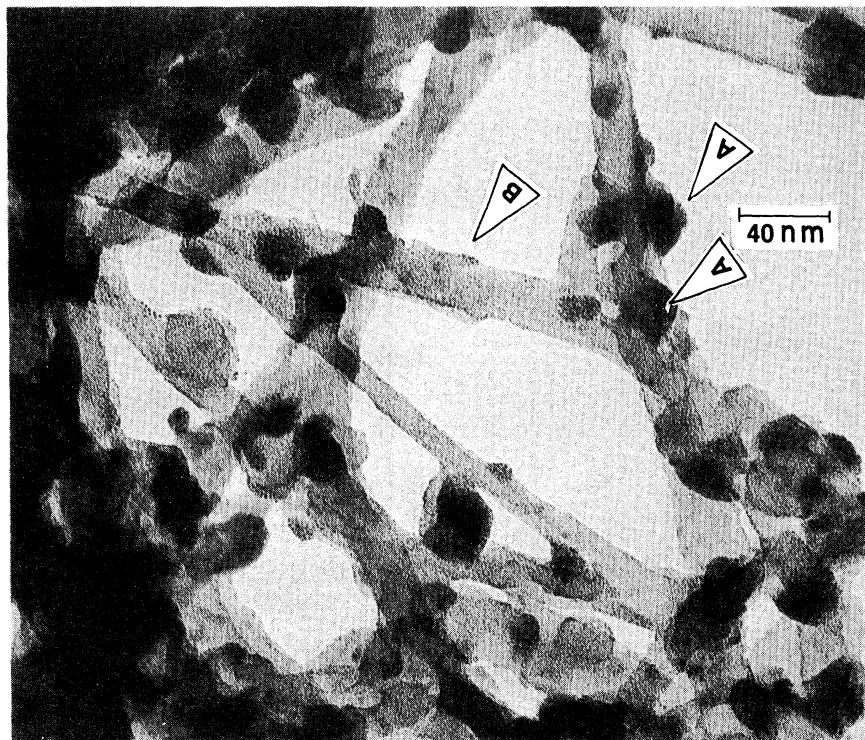


FIG. 5. High-resolution and -magnification electron micrograph of $\text{CH(IrCl}_6\text{)}$, showing two scales of dopant inhomogeneity, indicated by arrows *A* (large-scale inhomogeneity) and *B* (small-scale inhomogeneity).

remainder of the fibrils. If we assume that charge is transported between heavily doped regions, the small $\approx 15\text{-\AA}$ features are the significant contributors to charge transport. A detailed analysis of island size is important for determining the conduction model. The model of Sheng, for example, requires a distribution of island sizes. Our micrographs are not of sufficient resolution to make a histogram of island sizes.

$$\rho = \rho_0 \exp \left[\frac{4C}{k_B T} \right]^{1/2}, \quad (4)$$

then the metal-to-semiconductor transition can be seen in Fig. 6 as the concentration y , where the activation energy C curve changes slope. Data for $\text{CH}(\text{IrCl}_6)_y$ fit Eq. (4) for both *cis* and *trans* starting material.

The case of $\text{CH}(\text{FeCl}_3)_y$ has proved more difficult to classify. Behaviors fitting both Eqs. (2) and (3) have been observed, as well as exponents intermediate between $\frac{1}{4}$ and $\frac{1}{2}$. There were no obvious trends in behavior of the exponent on y . It appears, then, that two conduction mechanisms are acting in parallel in the case of $\text{CH}(\text{FeCl}_3)_y$.

IV. MATERIALS CHARACTERIZATION

To date, all electron-microscopic studies to elucidate the nature of the dopant distribution in polyacetylene have been carried out at a scale orders of magnitude larger than the smallest morphological subunits.¹⁶⁻¹⁸ Since fibrillar polyacetylene has a loose spongelike morphology, it is important to study the distribution of the dopant species in the individual fiber itself and any overgrowth thereof. The homogeneity (or lack of it) of dopant distribu-

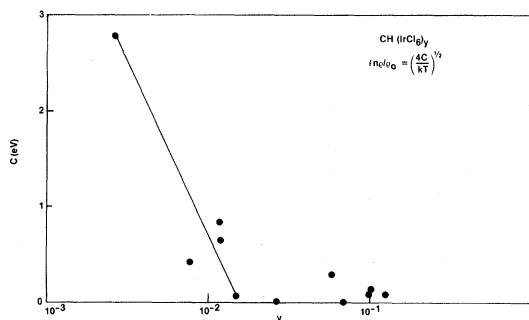


FIG. 6. Charging-energy parameter C as a function of dopant concentration y in $\text{CH}(\text{IrCl}_6)_y$.

tion can be studied through electron-microscopy techniques by taking advantage of the phase contrast produced by the heavier atoms present in the dopant species due to their larger atomic scattering factors. Thus this technique is ideally suited for the dopant of our choice $\text{H}_2\text{IrCl}_6 \cdot 6\text{H}_2\text{O}$ owing to the presence of the transition element Ir.

It should also be mentioned that this dopant has proved ideal for elucidation of the polyacetylene morphology for the same reason. Usual staining agents such as OsO_4 used to identify disordered regions of a nominally unsaturated polymer cannot be used in the case of polyacetylene, for it will indiscriminately chemically react with available double bonds in all regions. $\text{H}_2\text{IrCl}_6 \cdot 6\text{H}_2\text{O}$, on the other hand, will diffuse preferentially into disordered regions and will act as an effective staining agent by forming a charge-transfer complex with the polyacetylene chain.

Since we want to investigate the dopant distribution in the bulk synthesized "gel" polyacetylene, doping was carried out in solution using nitromethane as the solvent for the dopant. Fragments from this soft gel were transferred onto electron-microscopic grids which were subsequently dried on a vacuum line. All necessary precautions were taken to avoid exposure of the sample to air before introducing into the electron microscope (Phillips EM 400-T).

Figure 4 is an electron micrograph of iodine-doped *cis*-polyacetylene. The sample was heavily doped with iodine, the presence of which has been established by the backscattered x-ray spectra. The conductivity of the bulk sample, fragments from which yielded this micrograph, indicates the doping level to be above the semiconductor-metal transition. No segregation of dopants is evident to as small a scale as 30 \AA .¹⁹ The same observation is made for lightly-iodine-doped samples and for polyacetylene that was grown directly on electron-microscope grids and for *trans*-polyacetylene doped with iodine.

On the other hand, the distribution of the dopant species for the H_2IrCl_6 -doped polyacetylene (Fig. 5) is much more heterogenous. Aggregation and higher concentration in the lamellar overgrowth regions is indicated by the two arrow *A*'s. One naturally expects a higher degree of disorder and the presence of "fold surfaces" in such regions. Uneven texture along and across the fibers is also seen in Fig. 5, indicated by arrow *B* in contrast to iodine-doped polyacetylene in Fig. 4.

In spite of the heterogeneity of the dopant distributions, no clustering of free metallic iridium or its

salts is seen in the micrographs if proper washing procedures are employed. The presence of iridium as well as chlorine can be detected from the back-scattered x-ray spectra. While the relative stoichiometric abundance of these two species cannot be estimated by this procedure without proper calibration, it seems to remain invariant over large areas. Thus these results are complementary to the elemental analysis and compensation studies to be discussed later in this section.

In order to understand the conduction mechanism in doped polyacetylene, it is important to identify the dopant species and determine the nature of its interaction with the conjugated backbone of polyacetylene.

As mentioned in Sec. III, when polyacetylene is doped with halogens such as iodine and bromine, the species that is actually incorporated in the polymer is in the form of a polyhalide anion (i.e., I_3^- , I_5^-).¹¹ It is interesting to note that chlorine, which is too aggressive chemically to effectively dope polyacetylene, also forms the least-stable interhalogen compounds of the X_3^- type.

In the case of polyacetylene doped with AsF_5 , depending upon the doping and handling conditions, it is possible to obtain an arsenic-to-fluorine ratio of 1:5 or 1:6.²⁰ The former case represents the incorporation of AsF_5 or the protonic acid $HAsF_5OH$ and the latter results from the AsF_6 species. This illustrates some of the peculiarities associated with dopants that contain hydrolyzable halogen. We have found using elemental analysis that polyacetylene doped with $H_2IrCl_6 \cdot 6H_2O$ also contains hydrolyzed species of the form $IrCl_5OH$ and $IrCl_4OH_2$ with various amounts of coordinated H_2O . Furthermore, using spectrophotometric techniques, we have also observed the presence of these hydroxychloroiridates in the doping solution and therefore conclude that any chemistry involving the Ir-Cl bond has occurred before the polymer interacts with the dopant species.²¹ We believe that the active dopant species is a protonic acid such as $(H_3O)_2^+(IrCl_6)^{2-} \cdot (H_2O)_y$ or a hydrolyzed species thereof and that oxidation of polyacetylene occurs via the protonic acid mechanism (the exact mechanism has yet to be elucidated).

Figure 7 shows the absorption data for a thin film of undoped *cis*-polyacetylene (curve 1), doped to various levels with the iridium salt (curves 2 and 3), and after compensation with NH_3 (curve 4). As is expected for polyacetylene exposed to a dopant, there is a decrease in the strong $\pi \rightarrow \pi^*$ transition centered around 550 nm in the undoped polymer and the occurrence of a broad absorption extending

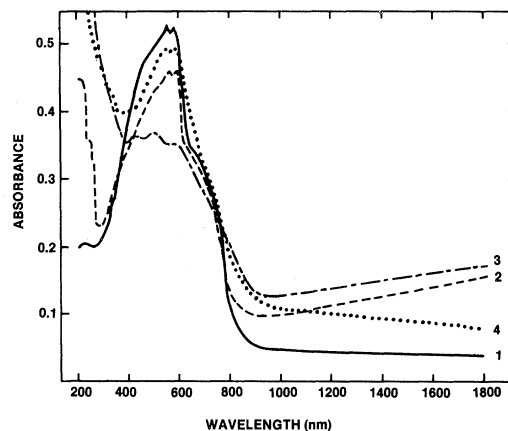


FIG. 7. Absorbance as a function of wavelength for $CH(IrCl_6)_y$ for undoped polyacetylene (curve 1) doped with $IrCl_6$ (curves 2 and 3) and after compensation with NH_3 (curve 4).

into the near-infrared portion of the spectrum. Both of these spectral changes have also been observed with I_2 , AsF_5 , and Br_2 as the dopant.²² The low-energy absorption has been interpreted as either the formation of a midgap soliton level²³ or as the dielectric anomaly due to metallic grains imbedded in a dielectric matrix.²⁴ Details of the absorption centered about 500 nm indicate that *cis* to *trans* isomerization is not complete at the dopant levels illustrated in Fig. 7.

Also note the occurrence of another new absorption peak below 300 nm which increases in intensity with increasing dopant concentration. This can be assigned to the strong $Cl \rightarrow Ir$ charge-transfer transition present in the hexachloroiridate anion.²⁵ When the doped sample is exposed to NH_3 gas, the near-infrared absorption disappears and the $\pi \rightarrow \pi^*$ transition returns to approximately its original intensity. The conductivity of the film drops precipitously during this compensation procedure and returns to the original insulating value for undoped polyacetylene (the same result was obtained with polyacetylene gels doped with the iridium salt). These results demonstrate that conduction in doped polyacetylene is due to charge carriers generated by the polymer-dopant interaction and not by free iridium metal or iridium salts incorporated during the solution doping. We also find no evidence of metallic iridium in our x-ray diffraction studies or electron-microscopic studies.

X-ray diffraction studies of $CH(I)_y$ and $CH(IrCl_6)_y$ indicate that the dopant induces disorder into the polyacetylene as measured by the full width at half maximum (FWHM) of the main dif-

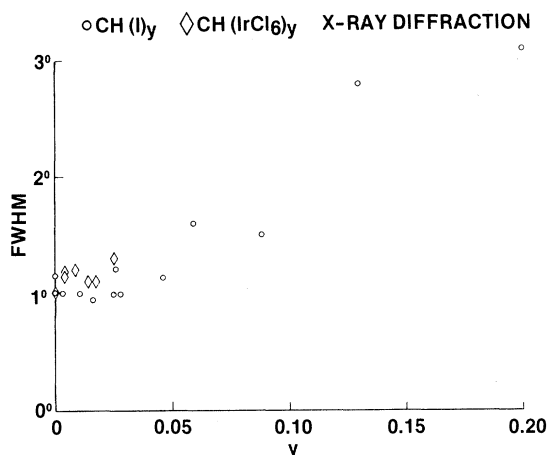


FIG. 8. Full width at half maximum of the x-ray peak at (nominally) 3.7–3.8 Å in $\text{CH}(\text{I})_y$ and $\text{CH}(\text{IrCl}_6)_y$.

fracted peak which reflects a periodicity of 3.7–3.8 Å, as shown in Fig. 8. At the dopant levels at which the metal-to-semiconductor transition occurs, there is no increase in the FWHM. Note that since I occurs as I_3^- a dopant level of 0.03 for $\text{CH}(\text{I})_y$ is comparable to a dopant level of 0.01 for the iridium chloride dopant. The position of the diffracted peak, which moves from 3.8 to 3.7 Å as the dopant concentration increases, indicates the extent of *cis* to *trans* isomerization. Hsu *et al.*²⁶ have shown that *cis*-polyacetylene has a characteristic $d=3.8$ Å while for *trans*-polyacetylene, $d=3.72$ Å. However, the x-ray technique is not sensitive to partial isomerization. Thus our results indicate that isomerization of $\text{CH}(\text{I})_y$ is not *complete* until well above the metal-to-semiconductor transition. It does not clarify the question of the degree of dopant-induced isomerization at the 1–2 % level of doping.

V. CONCLUSION

We have demonstrated two types of behavior in doped polyacetylene. For iodine and bromine

dopants, the temperature dependence of the resistivity is $\log_{10}\rho \propto T^{1/4}$ and TEM studies of $\text{CH}(\text{I})_y$ show uniform distribution of dopant. In the case of the large, spherical molecular dopants IrCl_6 and AsF_5 , the temperature dependence of the resistivity is $\log_{10}\rho \propto T^{1/2}$. TEM studies of $\text{CH}(\text{IrCl}_6)_y$ indicate dopant agglomeration. In the case of FeCl_3 dopant, the temperature dependence of $\log_{10}\rho$ is intermediate between $T^{-1/2}$ and $T^{-1/4}$. We suggest different transport mechanisms in the two cases represented by I and Br dopants on the one hand and IrCl_6 and AsF_5 dopants on the other hand. They are variable range hopping and charging-energy-limited tunneling, respectively. We have found the electrical properties to be insensitive to doping speed and technique and to starting isomerization state.

What determines whether dopant molecules agglomerate in polyacetylene? We suggest that the dopant molecule size and shape plays a role. It has been noted²⁷ that the linear chain dopants, e.g., I_3^- , may infiltrate the polymer as an intercalant, causing minimum disruption to the polymer chains. The larger spherical dopants may cause more disruption to the polyacetylene matrix, and it could be energetically favorable for the dopant molecules to nucleate.

ACKNOWLEDGMENTS

We are grateful to P. Cukor for his enthusiastic support and interest in this work. Skilled technical assistance from M. Knowles (electronics) and P. Cholewa and J. Georger, Jr. (chemistry) is gratefully acknowledged. X-ray analysis was provided by J. Mullins and M. Downey. Guidance and advice in the TEM work was provided by T. Emma. We thank M. Moore for many useful discussions about data analysis.

¹D. Moses, A. Denenstien, J. Chen, A. J. Heeger, P. McAndrew, T. Woerner, A. G. MacDiarmid, and Y. W. Park, *Phys. Rev. B* **25**, 7652 (1982).

²A. J. Epstein, H. Rommelmann, M. A. Druy, A. J. Heeger, and A. G. MacDiarmid, *Solid State Commun.* **38**, 683 (1981).

³K. Mortensen, M. L. W. Thewalt, Y. Tomkiewicz, T. C. Clarke, and G. B. Street, *Phys. Rev. Lett.* **45**, 490

(1980); Y. Tomkiewicz, T. D. Schultz, H. B. Brom, A. R. Taranko, T. C. Clarke, and G. B. Street, *Phys. Rev. B* **24**, 4348 (1981).

⁴G. E. Wnek, J. C. W. Chien, F. E. Karasz, M. A. Druy, Y. W. Park, A. G. MacDiarmid, and A. J. Heeger, *J. Polym. Sci. Polym. Lett. Ed.* **17**, 779 (1979).

⁵W. Deits, P. Cukor, M. Rubner, and H. Jopson, *J. Electron. Mater.* **10**, 683 (1981); E. K. Sichel, M. Knowles,

- M. Rubner, and J. Georger, Jr., *Phys. Rev. B* **25**, 5574 (1982).
- ⁶H. Shirakawa and S. Ikeda, *Polym. J.* **2**, 231 (1971); H. Shirakawa, T. Ito, and S. Ikeda, *ibid.* **4**, 460 (1973).
- ⁷S. Kivelson, *Phys. Rev. Lett.* **46**, 1344 (1981), and private communication; A. J. Epstein, H. Rommelmann, M. Abkowitz, and H. W. Gibson, *Phys. Rev. Lett.* **47**, 1549 (1981).
- ⁸Y.-W. Park, A. J. Heeger, M. A. Druy, and A. G. MacDiarmid, *J. Chem. Phys.* **73**, 946 (1980).
- ⁹N. F. Mott and E. A. Davis, *Electronic Processes In Non-Crystalline Materials*, 2nd ed. (Clarendon, Oxford, 1979).
- ¹⁰E. K. Sichel, M. Knowles, M. Rubner, and J. Georger, Jr., *Phys. Rev. B* **25**, 5574 (1982).
- ¹¹C. K. Chaing, Y. W. Park, A. J. Heeger, H. Shirakawa, E. J. Louis, and A. G. MacDiarmid, *J. Chem. Phys.* **69**, 5098 (1978).
- ¹²A. J. Epstein, H. W. Gibson, P. M. Chaikin, W. G. Clark, and G. Gruner, *Phys. Rev. Lett.* **45**, 1730 (1980).
- ¹³P. Sheng, B. Abeles, and Y. Arie, *Phys. Rev. Lett.* **31**, 44 (1973).
- ¹⁴E. Simanek, *Solid State Commun.* **40**, 1021 (1981).
- ¹⁵See, for example, T. Matsuyama, H. Sakai, H. Yamaoka, Y. Maeda, and H. Shirakawa, *Solid State Commun.* **40**, 563 (1981).
- ¹⁶M. Rolland, M. Aldissi, P. Bernier, M. Cadene, and F. Schue, *Nature* **294**, 60 (1981).
- ¹⁷M. Rolland, M. Cadene, J.-F. Bresse, A. Rossi, D. Riviere, M. Aldissi, C. Benoit, and P. Bernier, *Mater. Res. Bull.* **16**, 1045 (1981).
- ¹⁸A. J. Epstein, H. Rommelmann, R. Fernquist, H. W. Gibson, M. A. Druy, and T. Woerner, *Polymer* **23**, 1211 (1982).
- ¹⁹Epstein *et al.* make the same observation on the iodine distribution in a polyacetylene matrix on the basis of TEM measurements.
- ²⁰A. G. MacDiarmid and A. J. Heeger, *Chem. Scr.* **17**, 143 (1981).
- ²¹M. R. Rubner *et al.*, *J. Polym. Sci. Polym. Symp. Ed.* (in press).
- ²²C. R. Fincher, Jr., M. Ozaki, M. Tanaka, D. Peebles, L. Lauchlan, A. J. Heeger, and A. G. MacDiarmid, *Phys. Rev. B* **20**, 1589 (1979); M. Tanaka, H. Fujimoto, H. Yasuda, and J. Tanaka, *ACS Polymer Preprints* **23**, 91 (1982).
- ²³N. Suzuki, M. Ozaki, S. Etemad, A. J. Heeger, and A. G. MacDiarmid, *Phys. Rev. Lett.* **45**, 1209 (1980).
- ²⁴Y. Tomkiewicz, T. D. Schultz, H. B. Brom, A. R. Taranko, T. C. Clarke, and G. B. Street, *Phys. Rev. B* **24**, 4348 (1981).
- ²⁵P. K. Eidem, A. W. Maverick, and H. B. Gray, *Inorg. Chim. Acta* **50**, 59 (1981).
- ²⁶S. L. Hsu, A. J. Signorelli, G. P. Pez, and R. H. Baughman, *J. Chem. Phys.* **69**, 106 (1978).
- ²⁷G. B. Street and T. C. Clarke, *IBM J. Res. Dev.* **25**, 51 (1981).

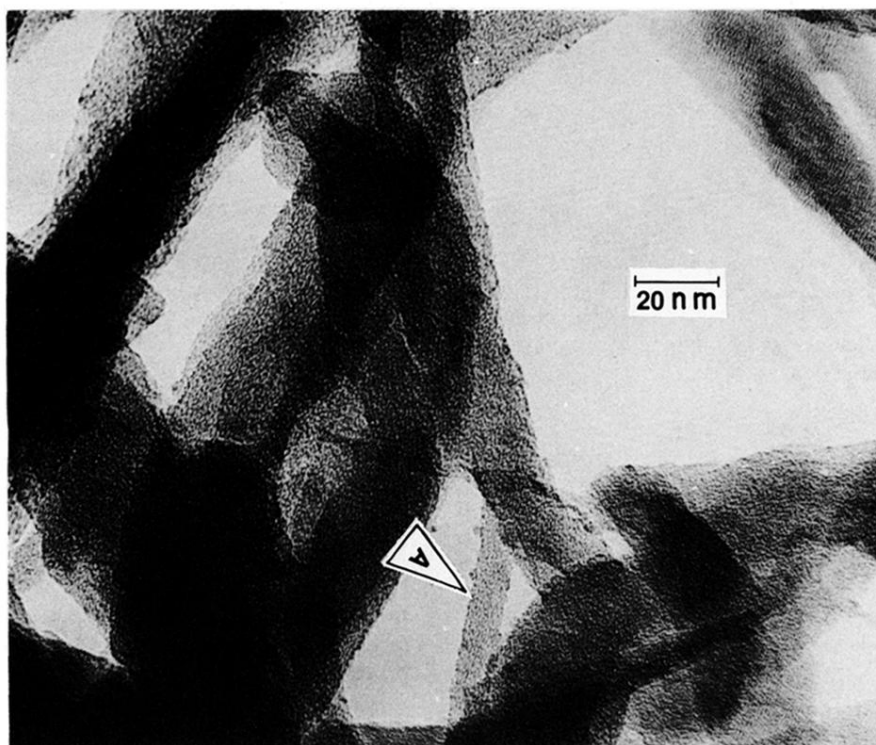


FIG. 4. High-resolution and -magnification electron micrograph of heavily doped CH(I), showing no evidence of dopant aggregation. Arrow indicates single fibril.

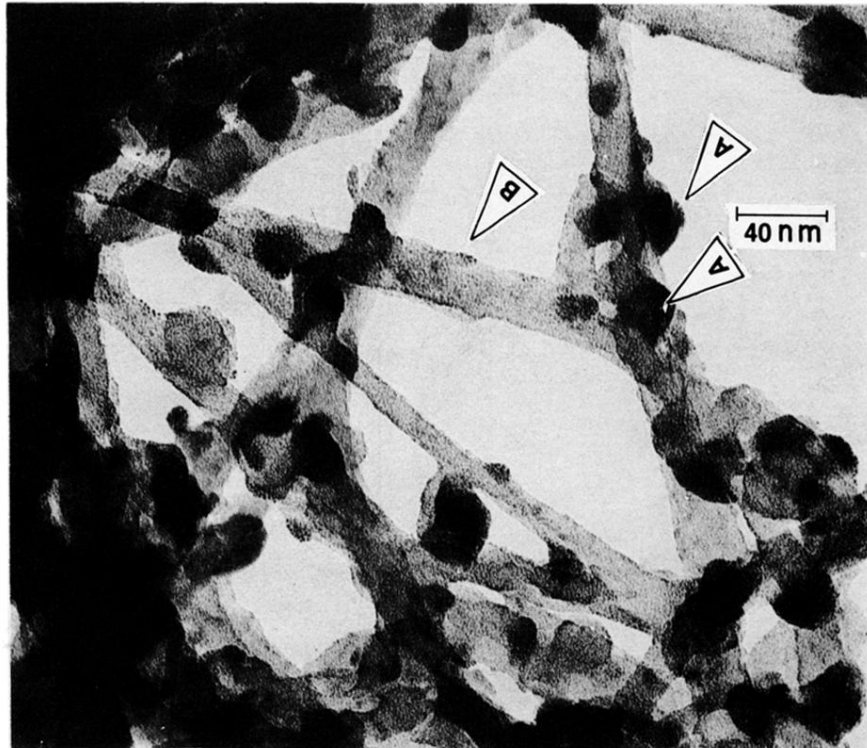


FIG. 5. High-resolution and -magnification electron micrograph of $\text{CH}(\text{IrCl}_6)_y$, showing two scales of dopant inhomogeneity, indicated by arrows *A* (large-scale inhomogeneity) and *B* (small-scale inhomogeneity).